Journal of Energy Storage 28 (2020) 101213

Contents lists available at ScienceDirect

Journal of Energy Storage

journal homepage: www.elsevier.com/locate/est

Self-reconfiguration batteries with stable voltage during the full cycle without the DC-DC converter

Feng Ji, Li Liao*, Tiezhou Wu, Chun Chang, Maonan Wang

Hubei Key Laboratory for High-efficiency Utilization of Solar Energy and Operation Control of Energy Storage System, Hubei University of Technology, Wuhan, 430068, China

ARTICLE INFO

Keywords:
Self-reconfigurable batteries
DC-DC converter
Cell balance
Lithium-ion batteries

ABSTRACT

This paper proposes the self-reconfigurable batteries topology without DC-DC converter, which is similar to self-reconfigurable batteries, but it can guarantee that the voltage of the battery pack is within the set range when the SOC (state of charge) is from 0 to 100%, even if the voltage will drop with the SOC or some cells will be bypassed. Simply put, when the battery pack is discharged, the batteries whose SOC is high and their voltages satisfy the demand are discharged, and the cell with lower SOC is continuously replaced, and the consistency of the battery pack is ensured while stabilizing the voltage. The topological and control strategy are analyzed in detail. The proposed topology is verified by the battery pack composed of 9 cells in series, the experiment result shows that this topology not only retains the advantages of good equalization of self-reconfiguration batteries but also maintains low voltage fluctuations even without DC-DC converters, besides, without the DC-DC converter, the capacity utilization rate of the battery pack reaches 99.8%, demonstrating the superior performance of the proposed topology.

1. Introduction

Lithium-ion batteries are widely used in a variety of applications, including electric vehicles, energy storage systems, due to their high energy density, long cycle life and low self-discharge rate [1]. A number of battery cells are usually connected in series in order to supply higher voltage and higher power to the load in a wide range of applications, while significant efforts are made by designers to select the battery cells such that they are as identical/matched as possible, the battery cells will still have mismatches in practice due to manufacturing tolerances, different self-discharge rates, uneven operating temperature across the battery cells, and nonuniform aging process, among others [2]. Such inevitable differences within battery cells will drift apart through cycling and could potentially lead to overcharging or over discharging, it is clear that such non-uniformity limits the battery capacity and may even cause safety issues [3]. Therefore, to properly maintain all cells balanced is of significant importance for enhancing battery life [4–6].

While the passive balancing dissipates the excess energy through resistors in the form of heat, the active balancing equalizes the battery cells by transferring the excess energy between battery cells [7]. Several active balancing systems have already been introduced [8–14], in addition, self-reconfigurable batteries are presented in the literature as an effective solution [15–18], however, the voltage of the self-reconfigurable batteries is relatively unstable, which is determined by the characteristics of the self-reconfigurable batteries (refer to Section 2), and the voltage of battery cell varies with SOC, for example, the NCM lithium-ion battery has a voltage range of 3.0 V–4.2 V, if the load is powered by 100 cells in series, the voltage range of the load is 300 V–420 V. Usually, the self-reconfigurable batteries and other equalization circuits need to be connected to the DC-DC converter to maintain the voltage of the battery pack, as shown in Fig. 1(a). Guertlschmid et al. presented in Ref. [19] a topology that deploys a power converter (DC-DC) for each battery cell, the cells are connected in series while the power converters are connected in parallel to each cell, as shown in Fig. 1(b). Huang et al. presented in Ref. [20] a topology that the cell and the DC-DC converter built a power unit, while the battery cells are decoupled, the power units are serially connected, as shown in Fig. 1(c).

Using the DC-DC converter is a relatively simple way, but it has energy loss and other deficiencies In order to stabilize the voltage of battery pack without the DC-DC converter, Kim et al. presented in Ref. [21] a topology that the cells can be dynamically configured in series and in parallel during operation to achieve the required voltage and current, respectively. Gunlu presented in Ref. [22] a topology that the cells can be connected in different configurations such as all of them serially, all of them in parallel, to obtain the required voltage.

* Corresponding author.
E-mail address: liliao513@163.com (L. Liao).

https://doi.org/10.1016/j.est.2020.101213
Received 12 October 2019; Received in revised form 18 December 2019; Accepted 10 January 2020

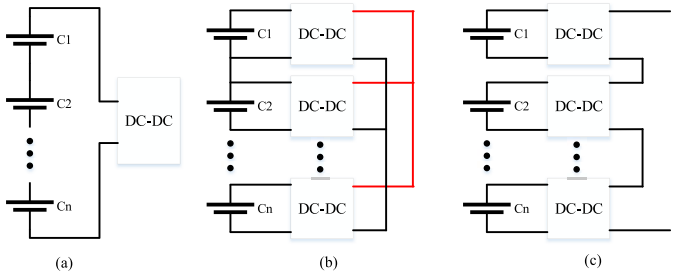

Fig. 1. Simplified diagram of the different self-reconfigurable batteries topologies with DC-DC converters (a) common method (b) Ref. [19] (c) Ref. [20].

Based on self-reconfigurable batteries, a novel self-reconfigurable equalization circuit without DC-DC converters is presented and the corresponding control strategy is proposed in this paper. The equalization circuitry is simple and easy to implement. A battery pack consisted of 9 cells in series is used for experience, during 0–20%, the voltage of the battery pack is 25.3 V–28.3 V without the DC-DC converter while the target voltage is 27 V, and the rang of SOC of the cell is within 1%, besides, the battery pack capacity utilization is 99.8%, the experience results show that the proposed equalization circuit has excellent performance.

The remainder of this paper is organized as follows. The working principle and shortcomings of self-reconfiguration batteries are introduced in Section 2. In Section 3, a detailed analysis of the equalization circuit and control strategy proposed in this paper. The characteristics of the equalizing circuit are introduced in Section 4. Experimental and analysis of experimental data are given in Section 5. Finally, the conclusion of this paper is given in Section 6.

2. Self-reconfigurable batteries

2.1. Working principle

In this section, we briefly introduce the working principle of self-reconfigurable batteries and analyze its shortcomings, a detailed analysis of self-reconfigurable batteries can be referred to [23–25].

As shown in Fig. 2, the self-reconfigurable batteries consist of n cells and 2n switches, each cell is connected to two switches. By controlling the two switches ON or OFF, the cell can be bypassed or connected to the battery pack to achieve battery pack equalization.

If the battery pack is discharged, as shown in Fig. 3(a), the SOC of cell 1 is the lowest, followed by that of cell 2, the SOC of cell 3 is relatively high, and the SOC of cell 4 to cell n is the same and higher than that of cell 1, cell 2 and cell 3. Although we assume that the SOC of cell 4 to cell n is the same, in fact, this is impossible. However, the battery pack allows a small inconsistency in the SOC of the cell, we can consider the cell in the range of permitted inconsistency of the battery pack to be consistent, which is simplified to be the same here.

Changing the switching state of the cell 1, cell 2 and cell 3, the switch in series with the cell is OFF (S12, S22, S32) and the switch in parallel with the cell is ON (S11, S21, S31), as shown in Fig. 3(b), cell 1, cell 2 and cell 3 are bypassed, while other cells are discharging until the time of Fig 3(c), the SOC of cell 3 is equal to that of cell 4 (cell 5 to cell n), and cell 3 is reconnected to the battery pack. Similarly, cell 2 is reconnected to the battery pack as shown in Fig. 3(d), and cell 1 is

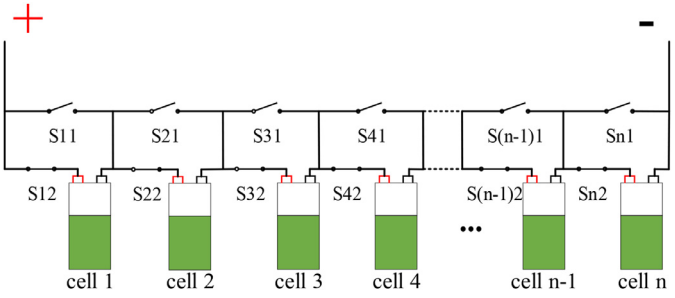

Fig. 2. Self-reconfigurable batteries topology.

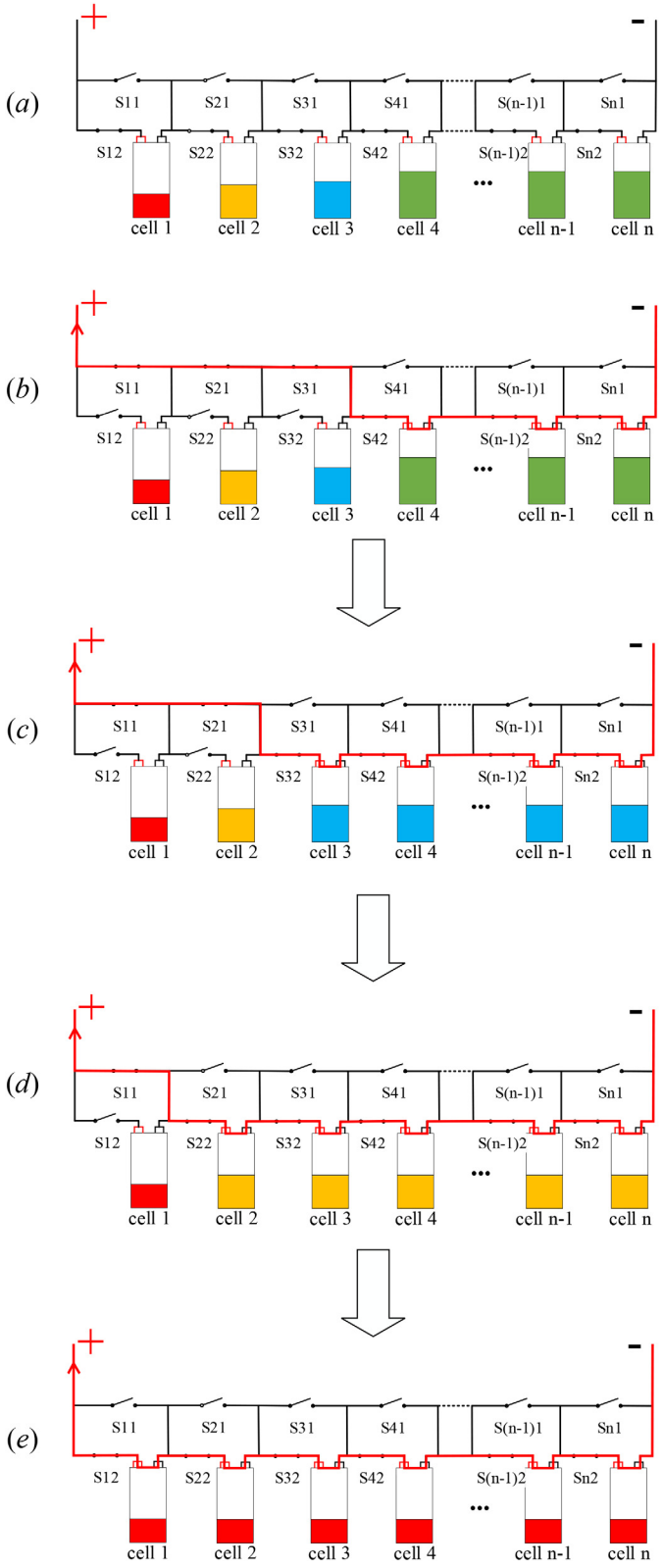

Fig. 3. Self-reconfigurable batteries equalization diagram (a) initial state, (b)–(e) equalization process.

Table 1
The voltage of the battery pack of Fig. 3(b) to (e).

	The voltage of the battery pack /V	The total voltage of 10 cells /V
Fig. 3(b)	25.9	36.3
Fig. 3(c)	28.8	35.7
Fig. 3(d)	31.5	34.8
Fig. 3(e)	33	33

reconnected to the battery pack as shown in Fig. 3(e).

The working principle of the self-reconfigurable batteries is that in the discharge phase, the cell with high SOC is always discharged (cell 4 to cell n in Fig. 3(b), cell 3 to cell n in Fig. 3(c), cell 2 to cell n in Fig. 3(d)), and the battery pack is equalized by reducing the discharge time of the cell with low SOC. In the same way, when the battery pack is charged, the cell can be equalized by reducing the charging time of the cell with high SOC

2.2. Disadvantages of self-reconfigurable batteries

As shown in Fig. 3(a), it is assumed that the battery pack is composed of 10 cells in series, that is, $n = 10$, the voltage of cell 1, cell 2, cell 3 and cell 4 are 3.3 V, 3.5 V, 3.6 V, and 3.7 V, respectively, then, the voltage of the battery pack of Fig. 3(b) to Fig. 3(e) are shown in Table 1.

Since the voltage of the cell will gradually decrease as the SOC, as shown in Table 1, even if all the cells are connected to the battery pack, the voltage between Fig. 3(b) (36.3 V) and Fig. 3(e) (33 V) is different, which exacerbates the voltage variation, and makes it is almost impossible to apply a circuit to a load that requires a higher voltage range unless the DC-DC converter is added.

3. Proposed battery equalization topology

Fig. 4 is the topology proposed in this paper, compared to Fig. 2, only the connection of the battery cell is changed, and some parallel cells are connected in series. It should be noted that we have not added or reduced the cells.

Assuming that the battery pack is composed of 90 cells, the self-reconfigurable batteries with DC-DC converter can be 30S3P, when the DC-DC converter realizes 3 times voltage conversion, as shown in Fig. 5(a). To obtain a higher voltage, the topology proposed in this paper needs to be connected 90 cells in series, that is, 90S1P, as shown in Fig. 5(b), the original 60 cells connected in parallel are all connected in series to obtain a higher voltage, that is, $m = 60$ in Fig. 4.

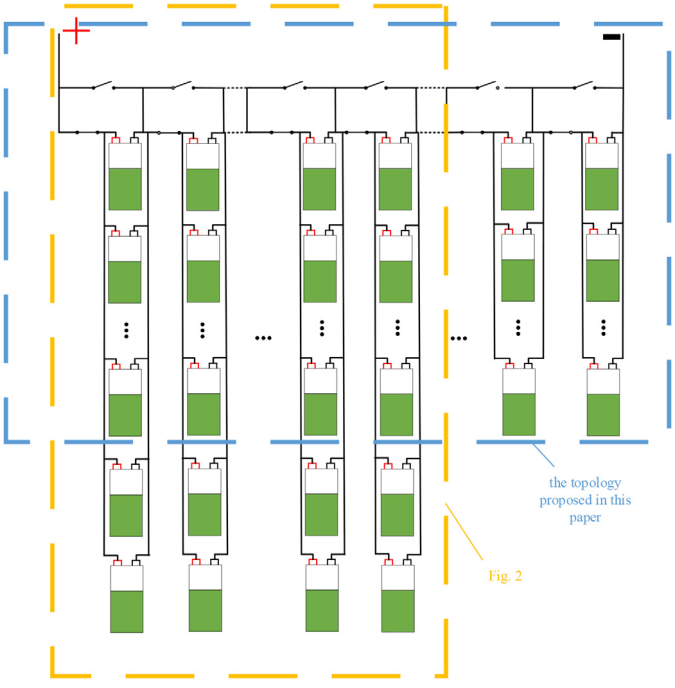

Fig. 4. The topology proposed in this paper.

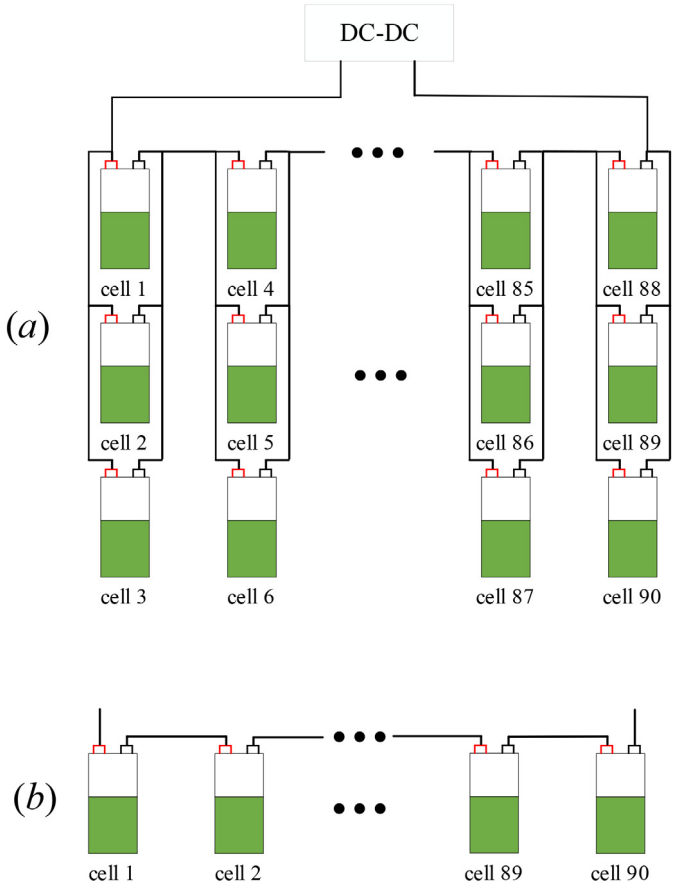

Fig. 5. Connection of 90 cells (a) traditional self-reconfigurable batteries (30S3P) (b) the topology proposed in this paper (90S1P).

3.1. Principle of stabilizing the voltage

To stabilize the voltage of battery pack at 120 V, as shown in Fig. 6, the battery pack consists of 40 cells in series, assuming that they are consistent, and the voltage of the cell in Fig. 6(a) to (d) is 4.0 V, 3.7 V, 3.4 V and 3.0 V respectively.

The voltage of the battery pack of Fig. 6(a) to (d) is shown in Table 2.

As shown in Fig. 6(a), the voltage of the cell is high, and only 30 cells need to supply power to the load. Since the voltage of all cells in the battery pack is the same, only the first 30 cells need to be selected to discharge, and the last 10 cells are bypassed. As shown in Fig. 6(b), to maintain the voltage, 32 cells are required, just like the previous analysis, the first 32 cells are selected to discharge, Fig. 6(c) and (d) can be deduced by analogy.

The topology proposed in this paper requires the number of cells connected in series m as shown in (1).

$$m \geq \frac{Ut}{Uc} \tag{1}$$

Where U_t is the target voltage of the battery pack, U_c is the discharge cut-off voltage of the cell, and for NCM battery, its discharge cut-off voltage is 3.0 V, that is, U_c is 3.0 V.

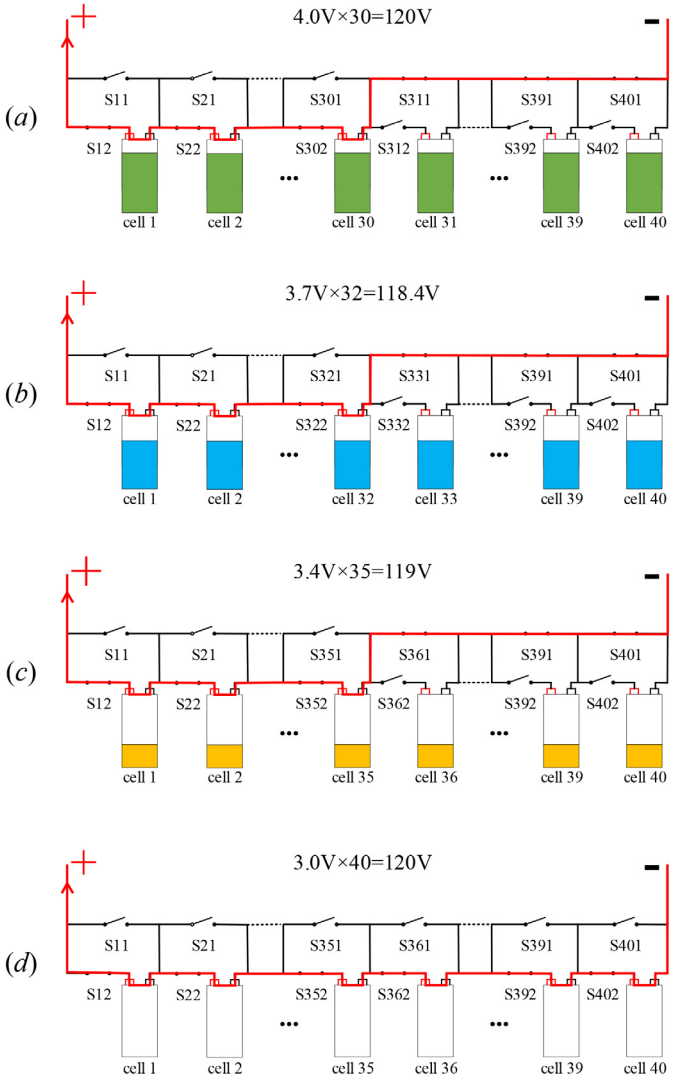

Fig. 6. Voltage stabilizing principle of the topology (a) powered by 30 cells, (b) powered by 32 cells (c) powered by 35 cells (d) powered by 40 cells.

Table 2
The voltage of Fig 6(a) to (d).

	Cell voltage/V	Number of cells	The voltage of battery pack/V
Fig. 6(a)	4.0	30	120
Fig. 6(b)	3.7	32	118.4
Fig. 6(c)	3.4	35	119
Fig. 6(d)	3.0	40	120

3.2. Control strategy

The above analysis only introduces the principle of circuit stability voltage but ignores cell equalization. In this section, we will introduce the control strategy of the proposed circuit through Figs. 7 and 8, so that the battery pack can maintain the SOC consistency of cells in the battery pack while stabilizing the voltage.

If the battery pack is discharged, as shown in Fig. 7, the SOC of the cell 1 to cell 3 is the same and highest, the SOC of the cell 4 to cell 6 is the same and medium, and the SOC of the cell 7 and cell 8 is the same and lowest.

Assuming that cell 1 to cell 6 can meet the battery pack voltage requirements, then they will be connected in series to the battery pack, and the remaining 2 cells with the lower SOC are bypassed (as shown in Figs. 7(a) and 8). After a while (as shown in Fig. 7(b)), the difference between the SOC of the cell 5 (cell 6) and the cell 7 (cell 8) satisfies the (2) and reaches the set condition, at this time, the first judgment condition in Fig. 8 is true, cell 5 and 6 are bypassed, cell 7 and cell 8 are connected to the battery pack (as shown in Fig. 7(c)).

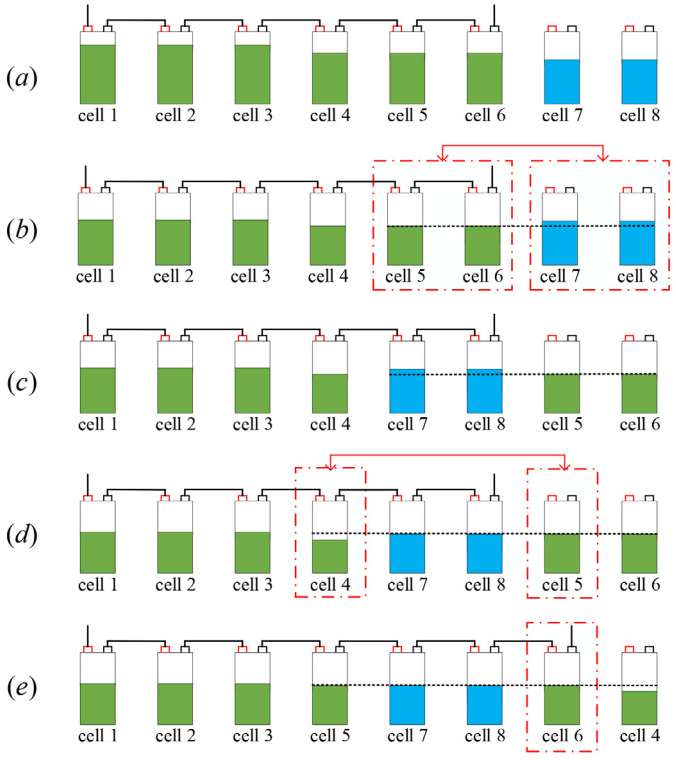

Fig. 7. Control strategy based on the proposed circuit (a) initial state, (b)-(e) equalization process.

$$SOC7 - SOC5 \geq SOCset \tag{2}$$

Where SOC_{set} is the difference in SOC. Similarly, as shown in Fig. 7(d), after a while of discharge, the difference between the SOC of cell 4 and cell 5 reaches a set threshold, the cell 4 is bypassed and the cell 5 is connected to the battery pack, as shown in Fig. 7(e), cell 6 is connected to the battery pack, because the cell 6 connected to the battery pack will make the voltage of battery pack more close to the set voltage (the second judgment conditions in Fig. 8), it should be noted that this is a hypothetical situation to facilitate the introduction of the working principle of the circuit.

From the analysis of Figs. 7 and 8 that even if there is a large inconsistency in the initial SOC of each cell in the battery pack (as shown in Fig. 7(a)), after a while, the SOC consistency of the battery pack is significantly improved (as shown in Fig. 7(e)). As analyzed in Fig. 3, this is because the battery cell discharged is always the cell with high SOC in the battery pack, and the cell with low SOC is bypassed, but unlike the traditional self-reconfigurable batteries, refer to (1), because of the extra batteries in series, when the cell with low SOC is bypassed, the cell with high SOC can replace the bypassed cell to supply power to the load, so as to keep the voltage of battery pack within the set range.

4. Analysis of the topology proposed in this paper

4.1. When the cell reaches the discharge cut-off voltage

Since the topology proposed in this paper has no DC-DC converter, the voltage provided by the battery pack for the load is the sum of all available cell voltages. As shown in Fig. 9, when the cell 6 to the cell 8 reach the discharge cut-off voltage and the cell 1 to the cell 5 are not

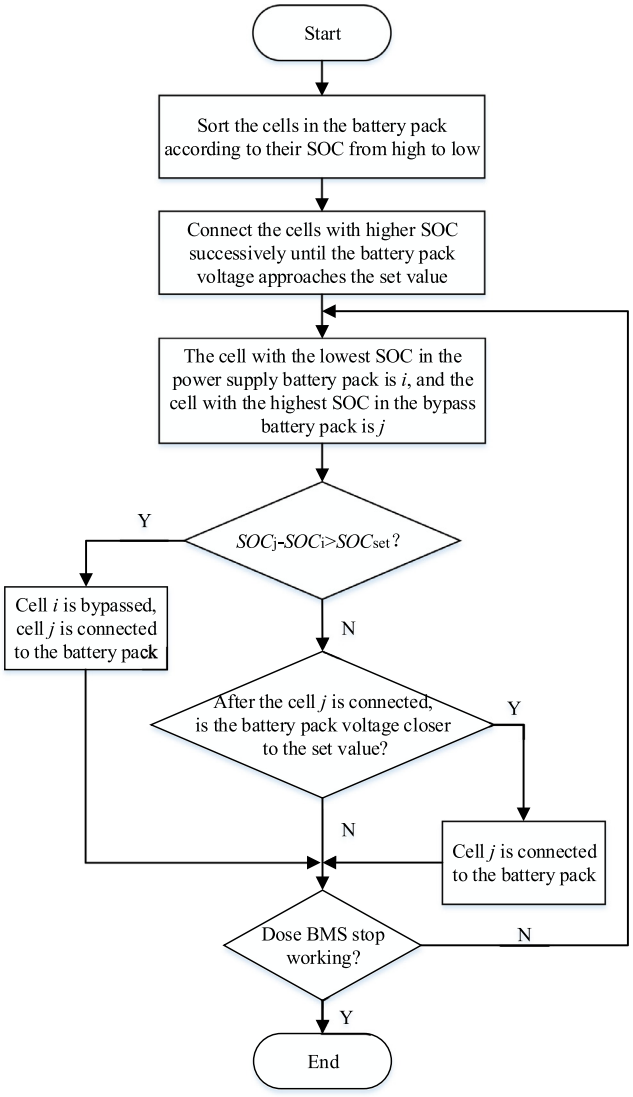

Fig. 8. Control flow chart.

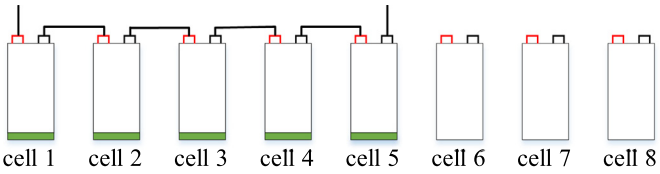

Fig. 9. When the cell 6 to the cell 8 reach the discharge cut-off voltage and the remaining cells are not available.

available, if the total voltage of cell 1 to cell 5 cannot meet the minimum voltage required by the load, the capacity of these cells cannot be released, resulting in a lower battery pack capacity utilization.

Refer to (2), the maximum SOC in Fig. 9 is not greater than the SOC_{set}, that is, when the SOC_{set} is larger, although the number of operations of the switching device in the circuit can be reduced, the available capacity of the battery pack may be low. However, when the SOC_{set} is smaller, although the available capacity of the battery pack can be better utilized, the number of operations of the switching device increases. Therefore, to solve the defect reflected in Fig. 9, only need to set the SOC_{set} to be large when the SOC of battery pack is high, so as to reduce the number of operations of the switching device, when the SOC of battery pack is low, the SOC_{set} is set to be small to fully utilize the available capacity of the battery pack.

4.2. The influence of the topological proposed in this paper on the cell

As shown in Fig. 5, although the cells are connected differently in Fig. 5(a) and (b), however, since the number of cells used in the battery pack is 90, the total energy stored in the battery pack is the same, and the total energy available for use is the same.

If the required power of the load is P, the currents I_1 and I_2 provided by each of the cells in Fig. 5(a) and (b) are as shown in (3) and (4), respectively.

$$I1 = \frac{P/\eta}{90 \times Ucell} \tag{3}$$

$$I2 = \frac{P}{90 \times Ucell} \tag{4}$$

Where η is the conversion efficiency of the DC-DC converter, U_{cell} is the voltage of cell, and we assume that the voltages of all the cells are the same. Refer to (3) and (4) that the current of each cell in Fig. 5(a) is slightly higher than that of Fig. 5(b), because of the power loss of the DC-DC converter, making the battery pack need to provide higher power to meet the load's power demand.

Although the proposed topology connects the originally parallel cells in series, it can be seen from the above analysis that this has little impact on the performance of the battery pack. However, it should be noted that the topology proposed in this paper usually supplies all the cells together when the battery pack is close to the cut-off voltage, but usually, some of the cells do not supply to the load. If the SOC is 100%, Fig. 5(a) is powered by 90 cells (the voltage of battery pack is 270 V), the topology proposed in this paper is only powered by 64 cells ($64 \times 4.2\ V = 268.8\ V$), the maximum power that the battery pack can provide is only 64/90 of Fig. 5(a). But the total energy that the battery pack can provide is the same because the battery pack is composed of 90 cells.

Therefore, when the power provided by the battery pack has some redundancy, the topology proposed in this paper can better achieve the goal of self-reconfigurable batteries with DC-DC converter and avoid the energy loss caused by the DC-DC converter. However, when the voltage required by the load is high, only the DC-DC converter can be used to match the load voltage.

5. Results and discussion

This paper chooses ICR 18650 lithium-ion battery produced by SAMSUNG for the experiment, whose nominal capacity and voltage are 2.2Ah and 3.7 V, respectively, it was produced in April 2018, and 9 cells are connected in series.

The MCU used in the experiment is STM32F407. To measure the voltage of the cell, the LTC6804 manufactured by Linear technology is used. This chip is powerful and can measure the voltage of 12 series-connected cells, the maximum error is 1.2 mV. ACS712-05 is used to measure the current. The switch components use the relay produced by SONGLE, which has the advantages of low conduction resistance, and its maximum conduction current is 10A, meeting the experimental requirements. It should be noted that this platform only verifies the rationality of the proposed topology, we can use semiconductor devices such as MOSFET instead of relays in the application such as electric vehicles, battery energy storage [21]. The load is replaced by a 100 Ω sliding rheostat, for convenience, the load is constant in experience. The EKF (Extended Kalman Filter) algorithm is used to estimate the SOC of each cell, which has the advantage of high estimation accuracy [26].The voltage, SOC, current and other information are displayed on a 3.2-inch TFT color screen. The equilibrium experimental platform is shown in Fig. 10.

Since the normal distribution of cell performance in the battery pack

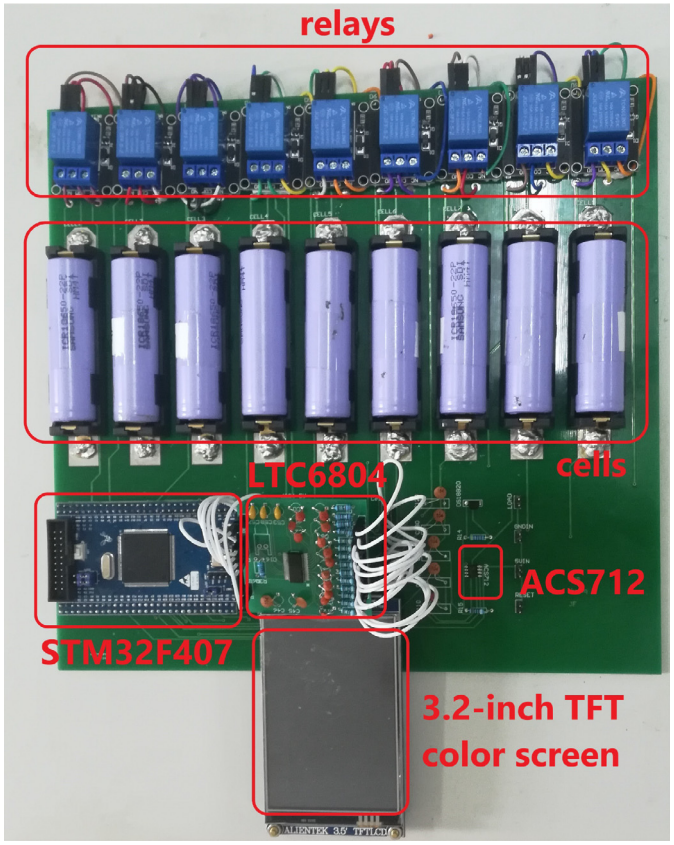

Fig. 10. Equilibrium experiment platform.

Table 3
Initial SOC of 9 cells.

	SOC/%
cell 1	51.5
cell 2	51.3
cell 3	51
cell 4	50.5
cell 5	50
cell 6	50
cell 7	49.3
cell 8	49.1
cell 9	49

[27,28], the initial SOC of 9 cells are shown in Table 3.

5.1. Cell balance and output voltage performance

The topology and control strategy proposed in this paper are used for experiments, where the target voltage of the battery pack is 27 V and SOC_{set} = 2% is considering the consistency of the battery pack. The SOC of each cell and the voltage of the battery pack are shown in Figs. 11 and 12, respectively.

As shown in Fig. 11, at the 60 s, cell 1 to cell 7 are discharged, while cell 8 and cell 9 are bypassed because the SOC of cell 8 and cell 9 is lower, and the voltage supplied by cell 1 to cell 7 is about 25.5 V, which is close to 27 V. At about 480 s, cell 7 (the lowest SOC in the power supply battery pack) is lower than cell 8 (the highest SOC in the bypass battery pack) 2% (SOC_{set}), cell 7 is bypassed and cell 8 is connected to the battery pack, since the SOC of cell 7 and cell 8 are similar, there is no change in the voltage of the battery pack at this time. At about 1140s, the battery pack has 8 cells instead of 7 cells connected in series, and the voltage of the battery pack rises to about 28.9 V, as shown in

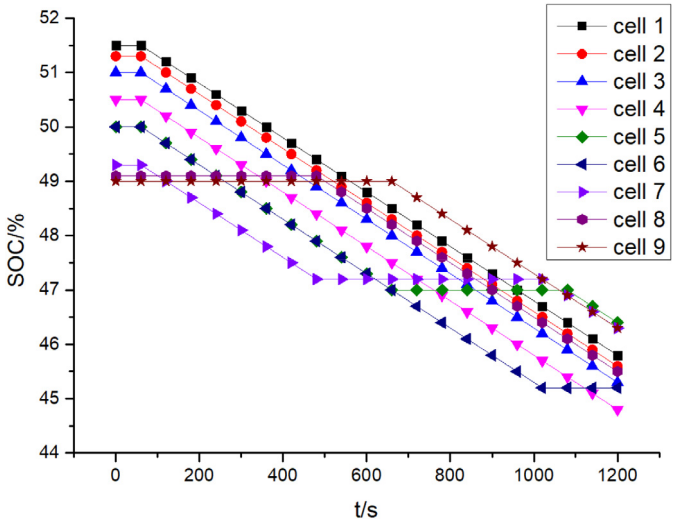

Fig. 11. The SOC of the topology proposed in this paper.

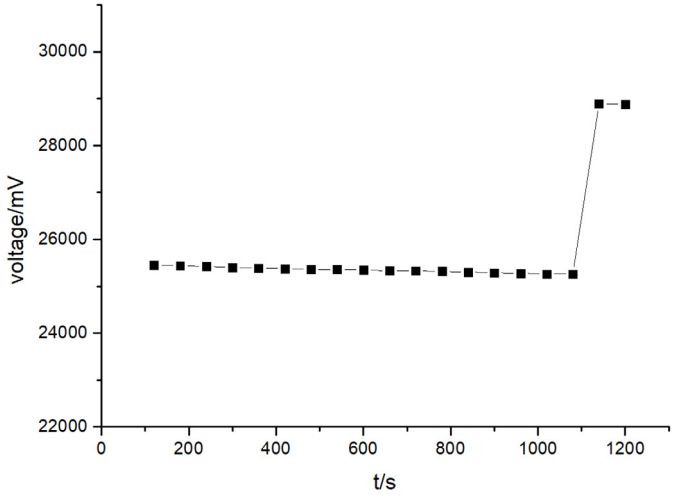

Fig. 12. The voltage of Fig. 11.

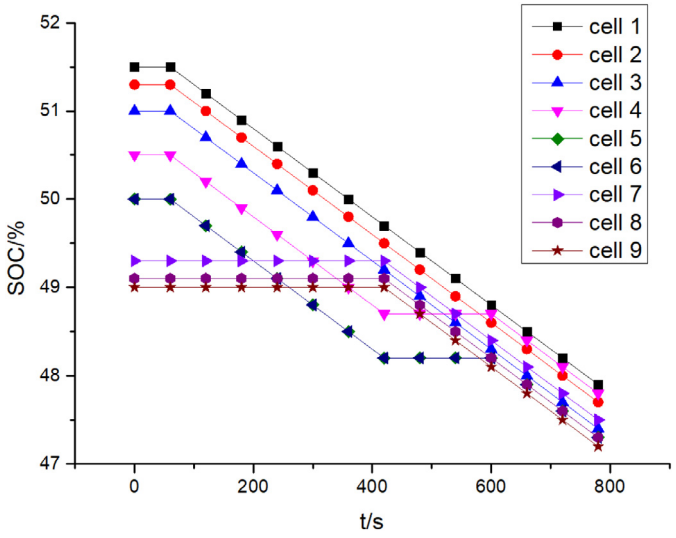

Fig. 13. The SOC of self-reconfigurable batteries.

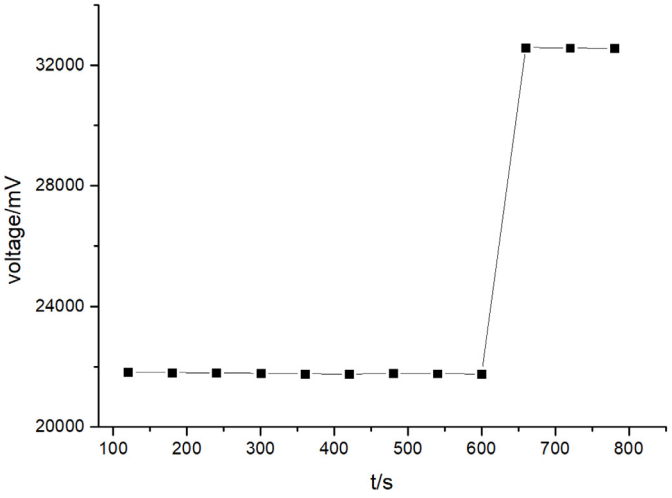

Fig. 14. The voltage of Fig. 13.

Fig. 12, because compared with 7 cells, if 8 cells are connected in series, the voltage of the battery pack is closer to 27 V (as shown in Fig. 7).

For the convenience of comparison, we conducted the experiment again with self-reconstructing batteries, as shown in Figs. 13 and 14, respectively.

As shown in Fig. 13, the battery pack starts to equalize after the 60 s, since the SOC of cell 7, cell 8 and cell 9 is low, these cells will be bypassed. that is to say, during the 60 s to 420 s, only cell 1 to cell 6 are discharged, as shown in Fig. 14, the voltage of the battery pack is about 22 V, however, the voltage of all the cells is about 33 V. At 420 s, the SOC of cell 7 to cell 9 reaches the set condition, cell 7 to cell 9 are connected to the battery pack and cell 4 to cell 6 are bypassed, as well as the analysis above, the voltage of the battery pack does not change much until about 600 s, the SOC of the 9 cells tends to be the same, cell 4 to cell 6 are connected to the battery pack, all the cells are discharged, and the voltage of the battery pack is the total voltage of all the cells of the battery pack, about 33 V.

As shown in Fig. 13, the range of self-reconfigurable batteries is reduced from 2.5% at the 60 s to 0.7% at 600 s, which better balances the battery pack, however, as shown in Fig. 11, the range of battery pack is reduced from 2.5% at 60 s to 1.6% at 1200 s, which is longer compared to self-reconfigurable batteries because the voltage of battery pack must be considered when bypassing the cell (the self-reconfigurable batteries bypasses 3 cells (Fig. 13) and the topology proposed in this paper bypasses 2 cells (Fig. 11)), so the number of cells bypassed is limited. Moreover, the topology proposed in this paper cannot make the battery pack as balanced as the self-reconfigurable batteries (Section 3).

Since the topology proposed in this paper is similar to the self-reconfigurable batteries, it has the advantages and disadvantages of self-reconfigurable batteries. However, as shown in Figs. 12 and 14, when the battery pack is discharged, compared with the self-reconfigurable batteries, the topology proposed in this paper can better stabilize the voltage of the battery pack and maintain the voltage of the battery pack within the set range, even if the cell is bypassed.

5.2. The capacity efficiency of the battery pack

As shown in Fig. 9, when the voltage of the battery pack is insufficient to meet the load voltage demand, the battery pack cannot continue to supply power to the load. To test the capacity utilization of the battery pack, the battery pack is discharged until it falls to the cut-off voltage, the initial SOC of the 9 cells is as shown in Table 4.

When the voltage of the battery cell in the battery pack is lower than 3.0 V, it is considered that the cell can no longer discharge. To increase the usable capacity of the battery pack, the SOC_{set} is 1% when the

Table 4
Initial SOC of the 9 cells when the battery pack drops to the cut-off voltage.

	SOC/%
cell 1	21
cell 2	21
cell 3	21
cell 4	20
cell 5	20
cell 6	20
cell 7	19
cell 8	19
cell 9	19

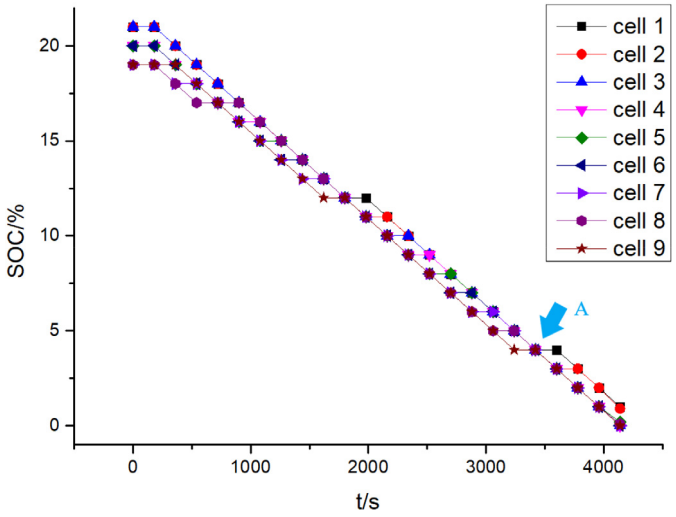

Fig. 15. The SOC of the topology proposed in this paper when the battery pack drops to the cut-off voltage.

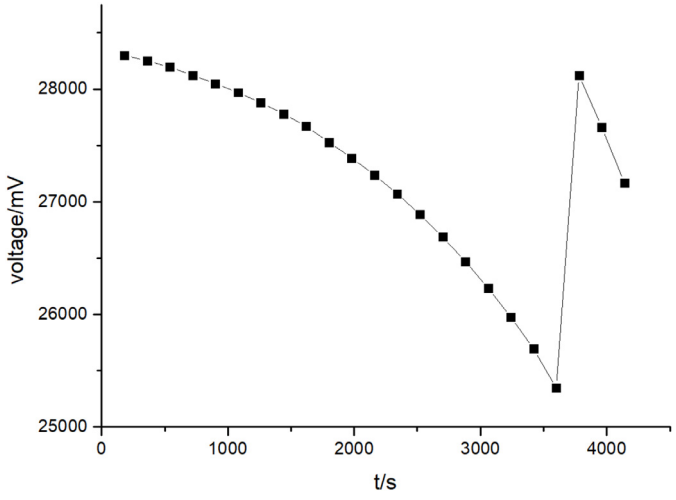

Fig. 16. The voltage of Fig. 15.

battery pack is discharged, The SOC of each cell and the voltage of the battery pack are shown in Figs. 15 and 16.

The analysis of Fig. 15 is the same as that of Fig. 11, and the details are not described here. However, it can be seen that the consistency of the battery pack is increasing from 0 s to about 1800 s, at the 1800 s, the SOC of 9 cells is almost the same, this also occurs at approximately 3400 s, as shown in point A of Fig. 15. In terms of voltage, since the SOC of 9 cells is low, in the beginning, 8 cells are discharged, and the voltage of the battery pack is about 28.3 V. However, compared with Fig. 12

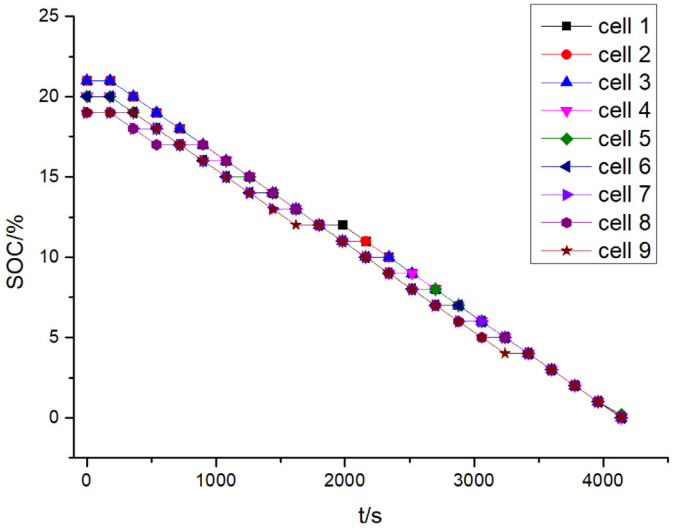

Fig. 17. The SOC of the topology proposed in this paper when the battery pack drops to the cut-off voltage (equilibrium at A).

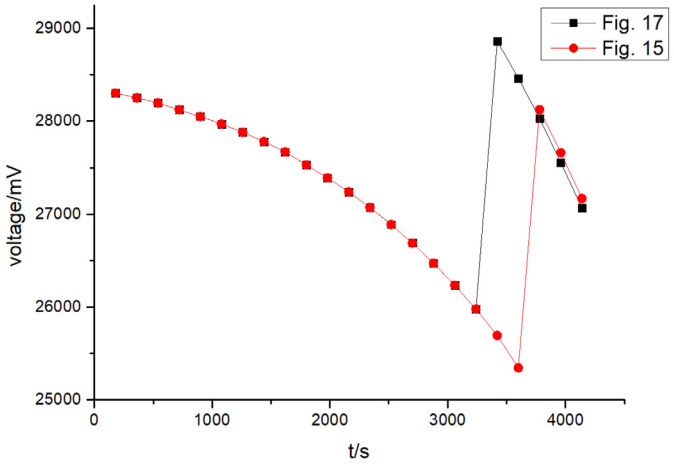

Fig. 18. The voltage of Figs. 15 and 17.

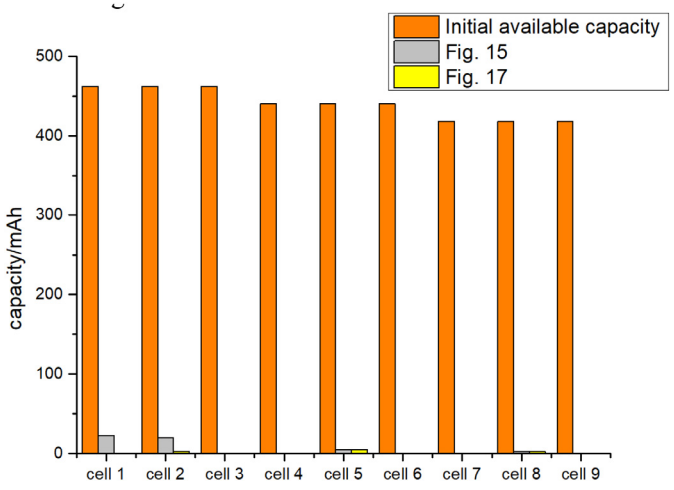

Fig. 19. The remaining capacity and initially available capacity.

and Fig. 14, the voltage drops rapidly in Fig. 16, this is because compared with SOC = 50%, the OCV varies with the SOC is larger when the SOC is 0 to 20%.

At point A in Fig. 15, we connect all the cells to the battery pack, the SOC and voltage are shown in Figs. 17 and 18, respectively.

Compared with Fig. 15, as shown in Fig. 17, about 3400 s, the SOC of the battery pack is almost uniform until the voltage of the battery cell is lower than 3 V, and although all the cells are discharged in advance, the available capacity of the battery can be better utilized, however, the voltage of the battery pack is increased, as shown in Fig. 18, about 3400 s, the voltage of the battery pack is close to 29 V.

In Figs. 15 and 17, the remaining capacity of each battery cell in the battery pack and its initial available capacity are shown in Fig. 19.

As shown in Fig. 19, the SOC of most cells drops to 0, the SOC of each battery cell is also less than 1% (SOC_{set}), and the initially available capacity of the battery pack is about 3960 mAh. In Fig. 15, the remaining available capacity of the 9 cells is about 48.4 mAh, the capacity utilization rate is about 98.8%, and in Fig. 17, the remaining available capacity of the 9 cells is about 8.8 mAh, and the capacity utilization rate is about 99.8%. However, it should be noted that the initial SOC of the battery pack is about 20% if the battery pack starts to discharge from 100%, the remaining available capacity of the 9 cells in Fig. 15 is also about 48.4 mAh, but the total available capacity will become 19800 mAh instead of 3960 mAh. The capacity utilization rate is 99.8% instead of 98.8%, the battery capacity utilization rate in Fig. 17 will be close to 100%.

At the end of the battery pack discharge, all the cells can be discharged when the battery packs tend to be consistent to maximize the available capacity of the battery pack, but in fact, the above target can be achieved by lowering the SOC_{set}, and as shown in Figs. 19, 15 and 17 of battery pack capacity utilization rate is not much different, and in most applications, the battery pack is rarely discharged to the cut-off voltage.

6. Conclusion

In this paper, a topology without DC-DC converter is proposed, which can not only ensure the consistency of the battery pack but also maintain the voltage of the battery pack during the use of the cell, the performance of the topology has been demonstrated experimentally. This topology can be widely used in applications where the power of the battery pack is redundant, because, for 3.7 V battery, the battery pack has a minimum of only 3/4.2 of the battery cell discharge, in addition, the optimal selection of SOC_{set} in Fig. 7 is related to the performance of the equalization system, this issue has been planned to be carried out in the future.

CRediT authorship contribution statement

Feng Ji: Writing - original draft, Methodology, Conceptualization. **Li Liao:** Software, Validation, Formal analysis. **Tiezhou Wu:** Project administration, Funding acquisition. **Chun Chang:** Software, Resources. **Maonan Wang:** Writing - review & editing.

Declaration of Competing Interest

The authors declare that they have no known competing financial interests or personal relationships that could have appeared to influence the work reported in this paper.

Acknowledgements

This work is supported by Hubei Provincial Major Technology Innovationproject of China (Grant No. 2018AAA056) and the Scientific Research Program of Hubei Provincial Department of Education (D20191402).

References

[1] F. Ju, W. Deng, J. Li, Performance evaluation of modularized global equalization

system for Lithium-ion battery packs, IEEE Trans. Autom. Sci. Eng. 13 (2) (Apr. 2016) 986–996.
[2] K.M. Lee, S.W. Lee, Y.G. Choi, et al., Active balancing of Li-ion battery cells using transformer as energy carrier, IEEE Trans. Ind. Electron. 64 (2) (Feb. 2017) 1251–1257.
[3] J. Wei, G. Dong, Z. Chen, System state estimation and optimal energy control framework for multicell lithium-ion battery system, Appl. Energy 187 (1) (Feb. 2017) 37–49.
[4] Y. Chen, X. Liu, Y. Cui, et al., A multiwinding transformer cell-to-cell active equalization method for Lithium-ion batteries with reduced number of driving circuits, IEEE Trans. Power Electron. 31 (7) (Jul. 2016) 4916–4929.
[5] M.Y. Kim, C.H. Kim, J.H. Kim, et al., A chain structure of switched capacitor for improved cell balancing speed of lithium-ion batteries, IEEE Trans. Ind. Electron. 61 (8) (Aug. 2014) 3989–3999.
[6] X. Zheng, X. Liu, Y. He, et al., Active vehicle battery balancing scheme in the condition of constant-voltage/current charging and discharging, IEEE Trans. Veh. Technol. 66 (57) (May 2017) 3714–3723.
[7] J. Qi, C. Lu D, A preventive approach for solving battery imbalance issue by using a bidirectional multiple-input Ćuk converter working in DCVM, IEEE Trans. Ind. Electron. 64 (10) (Oct. 2017) 7780–7789.
[8] X. Wang, K.W.E. Cheng, Y.C Fong, Series-Parallel switched-capacitor balancing circuit for hybrid source package, IEEE Access 6 (Jun. 2018) 34254–34261.
[9] L. He, Z. Yang, Y. Gu, et al., SoH-Aware reconfiguration in battery packs, IEEE Trans. Smart Grid 9 (4) (Jul. 2018) 3727–3735.
[10] X. Cui, W. Shen, Y. Zhang, et al., Novel active LiFePO4 battery balancing method based on chargeable and dischargeable capacity, Comput. Chem. Eng. 97 (1) (Feb. 2017) 27–35.
[11] F. Baronti, R. Roncella, R. Saletti, Performance comparison of active balancing techniques for lithium-ion batteries, J. Power Sources 267 (4) (Dec. 2014) 603–609.
[12] Y. Wang, C. Zhang, Z. Chen, et al., A novel active equalization method for lithium-ion batteries in electric vehicles, Appl. Energy 145 (1) (May 2015) 36–42.
[13] T.H. Phung, J. Crebier, A. Chureau, et al., Optimized structure for next-to-next balancing of series-connected lithium-ion cells, IEEE Trans. Power Electron. 29 (9) (Sep. 2013) 4603–4613.
[14] S. Wang, L. Shang, Z. Li, et al., Online dynamic equalization adjustment of high-power lithium-ion battery packs based on the state of balance estimation, Appl. Energy 166 (15) (Mar. 2016) 44–58.
[15] C. Song, N. Lin, D. Wu, Reconfigurable battery techniques and systems: a survey, IEEE Access 4 (1) (Mar. 2016) 1175–1189.
[16] T. Morstyn, M. Momayyezan, B. Hredzak, et al., Distributed control for state-of-charge balancing between the modules of a reconfigurable battery energy storage system, IEEE Trans. Power Electron. 31 (11) (Nov. 2016) 7986–7995.
[17] N. Bouchhima, M. Gossen, S. Schulte, et al., Life-time of self-reconfigurable batteries compared with conventional batteries, J. Energy Storage 15 (1) (Feb. 2018) 400–407.
[18] T. Kim, Q. Wei, L Qu, Series-connected self-reconfigurable multicell battery, Applied Power Electronics Conference & Exposition, 2011.
[19] M. Einhorn, W. Guertlschmid, T. Blochberger, et al., A current equalization method for serially connected battery cells using a single power converter for each cell, IEEE Trans. Veh. Technol. 60 (9) (Nov. 2011) 4227–4237.
[20] W. Huang, J.A.A. Qahouq, Energy sharing control scheme for state-of-charge balancing of distributed battery energy storage system, IEEE Trans. Ind. Electron. 62 (5) (May 2015) 2764–2776.
[21] T. Kim, W. Qiao, L. Qu, Power electronics-enabled self-x multicell batteries: a design toward smart batteries, IEEE Trans. Power Electron. 27 (11) (Nov. 2012) 4723–4733.
[22] G. Gunlu, Dynamically reconfigurable independent cellular switching circuits for managing battery modules, IEEE Trans. Energy Convers. 32 (1) (Mar. 2016) 194–201.
[23] N. Bouchhima, M. Schnierle, S. Schulte, et al., Active model-based balancing strategy for self-reconfigurable batteries, J. Power Sources 322 (1) (Aug. 2016) 129–137.
[24] E. Chatzinikolaou, J. Rogers D, Hierarchical distributed balancing control for large scale reconfigurable ac battery packs, IEEE Trans. Power Electron. 33 (7) (Jul. 2018) 5592–5602.
[25] M. Momayyezan, B. Hredzak, V.G. Agelidis, Integrated reconfigurable converter topology for high-voltage battery systems, IEEE Trans. Power Electron. 31 (3) (Mar. 2016) 1968–1979.
[26] J. Meng, M. Ricco, G. Luo, et al., An overview and comparison of online implementable soc estimation methods for lithium-ion battery, IEEE Trans. Ind. Appl. vol.54, (2) (Mar, 2018) 1583–1593.
[27] T. Baumhöfer, M. Brühl, S. Rothgang, et al., Production caused variation in capacity aging trend and correlation toinitial cell performance, J. Power Sources 247 (1) (Feb. 2014) 332–338.
[28] C. Campestrini, P. Keil, S.F. Schuster, et al., Ageing of lithium-ion battery modules with dissipative balancing compared with single-cell ageing, J. Energy Storage 6 (May. 2016) 142–152.